

# Potentiometric Mass Titrations: Experimental and Theoretical Establishment of a New Technique for Determining the Point of Zero Charge (PZC) of Metal (Hydr)Oxides

Kyriakos Bourikas, John Vakros, Christos Kordulis, and Alexis Lycourghiotis\*

Department of Chemistry, University of Patras, GR–26500 Patras, Greece, School of Science and Technology, Hellenic Open University, Sahtouri 16, GR–26222 Patras, Greece, and Institute of Chemical Engineering and High-Temperature Chemical Processes, FORTH/ICE-HT, P.O. Box 1414, GR–26500 Patras, Greece

Received: April 25, 2003; In Final Form: June 21, 2003

In this paper, we present a novel methodology, called the potentiometric mass titration (PMT) technique, for determining the point of zero charge (pzc) of mineral hydr(oxides) immersed in electrolytic solutions. Following PMT, the pzc is identified as the common intersection point (CIP) of the potentiometric curve of the blank solution with the corresponding curves of the impregnating suspensions containing different amounts of the immersed mineral (hydr)oxides. Full experimental results related to the determination of pzc using the PMT technique and four traditional techniques (potentiometric titrations, mass titrations, immersion, and micro-electrophoresis (for determining the isoelectric point, equal to pzc in cases where no specific adsorption takes place)) are presented for four oxides, namely, MgO,  $\gamma$ -Al<sub>2</sub>O<sub>3</sub>, TiO<sub>2</sub>, and SiO<sub>2</sub>. The comparison of the pzc values determined by PMT, with the corresponding ones determined using the traditional methodologies, strongly suggested that the PMT technique can be used to determine the pzc of oxides. A simulation procedure of the PMT technique has been developed and applied to model oxides with properly selected acid–base characteristics and to various combinations of models related to the charging mechanism of the oxide surface (1 site/1 pK, 1 site/2 pK, multisite models) and to the description of the interfacial region (diffuse double layer, constant capacitance, basic Stern models). The intensive application of this simulation procedure offered a quantitative interpretation of the methodology. Specifically, it was demonstrated that (a) the application of the “quick scan” version of the PMT technique, realized by recording the titration curve of the blank solution (pH vs  $V_{\text{added acid}}$ ) and the corresponding curve of a suspension of a given amount of the immersed oxide, indeed results in the determination of the pzc, provided that this is greater than a value of about 4; (b) the application of the “typical” version of PMT, realized by recording the titration curves of three different suspensions (pH vs  $V_{\text{consumed acid}}$ ) containing different masses of the immersed oxide, provides the pzc value of this oxide over the whole pH range; and (c) the CIP that is determined, using PMT, corresponds to the pzc irrespective of the charging mechanism of the oxide surface and the structure of the double layer developed between the oxide surface and the solution. However, in the case where the basic Stern model is used to describe the interfacial region, the pzc value determined by PMT deviates slightly from the true value when the value of the affinity constants of the ion pairs formed between the positive counterions and the surface is different than the corresponding value of the negative counterions.

## Introduction

In a previous preliminary communication, we reported a novel technique, called potentiometric mass titrations (PMT), for determining the point of zero charge (pzc) of solids in electrolytic solutions.<sup>1</sup> It is well known that the surfaces of solids, principally, of the mineral (hydr)oxides, are charged in electrolytic solutions, and this charge depends on the pH of the solution. The pzc is defined as the pH value where the surface charge is equal to zero, namely, the pH at which the charge due to the positive surface groups is equal to that due to the negative ones. In the absence of surface impurities or other charge-determining ions, the above-mentioned groups are the hydroxyl groups of the metal (hydr)oxide. The pzc is a very important parameter that plays a crucial role in many chemical phenomena such as adsorption, interactions between particles in colloidal suspensions, coagulation, dissolution of mineral

(hydr)oxides, electrochemical phenomena, and so forth. Moreover, it is characteristic of materials used as adsorbents in various processes. Finally, we should stress its significance and usefulness in studying the mineral–solution interface,<sup>2–4</sup> a region with great importance in aqueous environmental chemistry<sup>5–11</sup> as well as in the preparation of supported catalysts.<sup>12–21</sup>

The value of the pzc is related to the acidity constants of the surface groups, but the exact relationship depends on the model adopted for describing the acid–base behavior of a solid surface in electrolytic solutions (e.g., 1 site/1 pK, 1 site/2 pK, multisite model).

Following PMT, the pzc is identified as the common intersection point (CIP) of the potentiometric curve of the blank solution with the corresponding curves of the impregnating suspensions containing different amounts of the immersed mineral oxides. Therefore, one may easily determine the pzc either by recording two potentiometric titration curves—one for the blank solution and one for a suspension of a given amount

\* To whom correspondence should be addressed. E-mail: kmpo@chemistry.upatras.gr. Tel: +302610997143. Fax: +302610994796.

**TABLE 1: Various Surface-Charging Models and Electrostatic Models Adopted to Perform the Simulation Procedure<sup>a</sup>**

surface-charging model (abbreviation)	parameters	values <sup>b</sup>
1 site/1 pK model		
$\text{SOH}^{-1/2} + \text{H}^+ \xrightleftharpoons{K} \text{SOH}_2^{+1/2}$ (1)	$ \text{pK}  = \text{pzc}$	
	$N_s$	8 sites $\text{nm}^{-2}$
	SC	(1 g, 3 g, 7 g, 20 g, 100 g)/100 mL
	SSA	100 $\text{m}^2 \text{g}^{-1}$
1 site/2 pK model		
$\text{SO}^- + \text{H}^+ \xrightleftharpoons{K_1} \text{SOH}$ (2)	$( \text{pK}_1  +  \text{pK}_2 )/2 = \text{pzc}$	
$\text{SOH} + \text{H}^+ \xrightleftharpoons{K_2} \text{SOH}_2^+$ (3)		
	$N_s, \text{SC}, \text{SSA}$	as above
multisite model (Music)		
$\text{S}_i^{z_i} + \text{H}^+ \xrightleftharpoons{K_i} \text{S}_i\text{H}^{z_i+1}$ (4)	$\text{pK}_i, z_i, N_{s_i}$	
	SC, SSA	as above
electrostatic model		
diffuse double-layer model (DDL)	$I$	0.01 M $\text{KNO}_3$
constant capacitance model (CC)	$I$	0.01 M $\text{KNO}_3$
	$C$	1 F $\text{m}^{-2}$
basic stern model (BS) (in combination with 1 site/1 pK model)		
	$I, C$	as above
$\text{SOH}^{-1/2} + \text{C}^+ \xrightleftharpoons{K_C} \text{SOH}^{-1/2} - \text{C}^+$ (5)	$\text{pK}_C, \text{pK}_A$	
$\text{SOH}_2^{+1/2} + \text{A}^- \xrightleftharpoons{K_A} \text{SOH}_2^{+1/2} - \text{A}^-$ (6)		

<sup>a</sup> S: metal of the (hydr)oxide; K: protonation constants; Ns: site density; SC: solid concentration; SSA: space specific area;  $z_i$ : charge of the surface site  $\text{S}_i$ ; I: ionic strength; C: capacitance of the double layer;  $K_C, K_A$ : ion pair affinity constants of surface hydroxyls with the cations and anions of the electrolyte, respectively. <sup>b</sup> Values of the parameters used in all simulations. The values of the remaining parameters of the second column are illustrated in the corresponding Figure legends.

of the immersed oxide—or by recording the potentiometric titration curves of the suspension for three different values of the mass of the oxide immersed in the electrolytic solution. The former offers a quick scan for determining the pzc whereas the later offers more accuracy than the former.

The underlying idea on which the PMT technique has been based is that the immersion of a given amount of an oxide modifies the titration curve achieved for the blank solution at all pH values with the exception of that corresponding to the pzc. The deviation of the pH value achieved for the suspension from the corresponding one achieved for the blank solution, for a given value of the added acid in the suspension, is proportional to the amount of the immersed oxide. This is because the latest is, in turn, proportional to the number of surface sites responsible for the adsorption–desorption of the  $\text{H}^+$  ions.

To illustrate the PMT technique, we have reported four potentiometric titration curves for each one of four different oxides ( $\text{SiO}_2$ ,  $\text{TiO}_2$ ,  $\gamma\text{-Al}_2\text{O}_3$ , and  $\text{MgO}$ ) used in industrial catalysis as supports for preparing supported catalysts by dry or wet impregnation or equilibrium deposition filtration, otherwise called equilibrium adsorption.<sup>14</sup> The pzc values that were achieved were compared with the corresponding ones determined by using three widely used techniques for determining the pzc, namely, the potentiometric titrations technique (PT), the mass titration technique (MT), and the immersion technique (IT).<sup>22–26</sup> A first, rather qualitative interpretation has shown that the common intersection point provided by the PMT technique is indeed the pzc of an oxide.<sup>1</sup>

The purpose of the present full paper is twofold. First, we shall present experimental details and the full experimental results on which the PMT technique has been supported. In these

results, we include microelectrophoretic mobility measurements leading to the determination of the isoelectric point (IEP) because this parameter is equal to the pzc in cases where no specific adsorption takes place.<sup>27–29</sup> The second, most important, goal of the present work is to demonstrate *quantitatively* that the application of the PMT technique actually provides pzc values and to investigate whether the pzc values that are determined using PMT are independent of the surface ionization mechanism and the structure of the interface developed between the surface of the oxide particles and the impregnating suspensions. To achieve the second goal of the present investigation, we develop and apply a simulation procedure of the PMT technique.

## Experimental Section

**Materials.** Commercial  $\text{TiO}_2$  (Degussa, P25,  $\text{SSA} = 50 \text{ m}^2\text{g}^{-1}$ ),  $\text{SiO}_2$  (Alfa, amorphous fumed,  $\text{SSA} = 175\text{--}200 \text{ m}^2\text{g}^{-1}$ , 99.8% metal base 325 mesh), and  $\text{MgO}$  (Merck, pro analysis min 97%) were used in the present study. The  $\gamma\text{-Al}_2\text{O}_3$  that was used was prepared by adding  $\text{NH}_4\text{OH}$  to a solution of aluminum nitrate ( $\text{Al}(\text{NO}_3)_3 \cdot 9\text{H}_2\text{O}$ , Riedel de Haen analytical grade) at a constant pH equal to 10. The suspension was aged at  $25^\circ \text{C}$  for 5 h, and then it was filtered. The solid that was produced,  $\text{Al}(\text{OH})_3$ , was dried at  $110^\circ \text{C}$  for 24 h, and then it was air-calcined at  $500^\circ \text{C}$  for 5 h to be transformed into  $\gamma\text{-Al}_2\text{O}_3$ . The prepared  $\gamma\text{-Al}_2\text{O}_3$  was identified by XRD analysis.

The indifferent electrolyte solutions used in the PT, IT, MT, PMT, and microelectrophoresis were prepared by using  $\text{KNO}_3$  (Merck, analytical grade) dissolved in triply distilled,  $\text{CO}_2$ -free water.

**Potentiometric Mass Titrations and Potentiometric Titrations.** PMTs were performed, under an  $\text{N}_2$  atmosphere, for

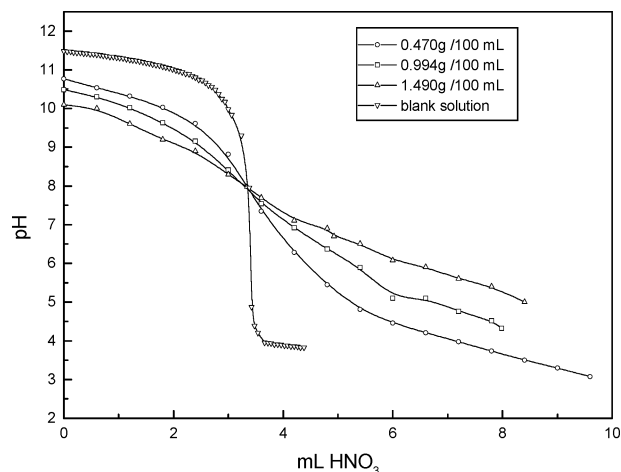


**Figure 1.** Experimental curves corresponding to the proposed potentiometric mass titrations technique for the determination of the pzc of  $\gamma$ - $\text{Al}_2\text{O}_3$ .

**TABLE 2: pzc Values of Several Oxides Measured Using Various Techniques**

oxide	method of measuring pzc values <sup>a</sup>				
	PT	MT	ME	IT	PMT
$\text{Al}_2\text{O}_3$	8.6	8.4	8.2	8	8.0
$\text{TiO}_2$	6.3	6.4	6.4	6	6.2
$\text{SiO}_2$	3.1	3.3	3.0	2.9	3.2
$\text{MgO}$	10.0	10.9	12.0	10.3	10.2

<sup>a</sup> All pzc values are measured using aliquots from the same sample of each oxide.

a blank solution and suspensions of three different masses of the immersed oxide at constant ionic strength (0.03 M) and temperature ( $25.0 \pm 0.1$  °C). PTs were performed, under an  $\text{N}_2$  atmosphere and constant temperature ( $25.0 \pm 0.1$  °C), for three suspensions having the same amount of the immersed oxide but different ionic strengths—0.001, 0.01, and 0.1 M. In both methodologies, the aqueous suspension containing a given amount of the immersed oxide was equilibrated for 20 h to reach an equilibrium pH value. A small amount of base, 1 M KOH, was then added to deprotonate a significant part of the surface sites, rendering the surface negative, and then the suspension was titrated by adding small volumes of a 0.1 or 0.5 M aqueous  $\text{HNO}_3$  solution. The pH value was recorded after each addition of the acidic solution as a function of its volume. A similar titrating procedure was followed for the blank solution.

The number of hydrogen ions consumed on the surface of the oxide,  $\text{H}^+_{\text{c}}$  ( $\mu\text{eq m}^{-2}$ ), at each pH value may be determined by subtracting the titration curve of the blank solution from the titration curve of the suspension. Details concerning the setup and the procedure that were used as well as the method of determining the surface charge,  $\sigma_o$ , have been reported elsewhere.<sup>30</sup>

**Mass Titrations.** MT were performed under an  $\text{N}_2$  atmosphere at constant ionic strength (0.03 M) and temperature ( $25.0 \pm 0.1$  °C) following the method proposed by Noh and Schwarz.<sup>22</sup> The aqueous suspensions, containing different amounts of the immersed oxide, were equilibrated for 20 h to reach an equilibrium pH value. The pH of each suspension was then measured using a digital pH meter (Metrohm) standardized by NBS buffers. The pzc is easily determined from the appearance of a plateau in the curve “pH vs mass”.

**Immersion Technique.** A number of aqueous solutions of indifferent electrolyte (blank solutions) of varying pH were prepared, and a small amount of the oxide was added to each

of these solutions. The aqueous suspensions were equilibrated for 20 h to reach an equilibrium pH value. The pH of each suspension was then measured using a digital pH meter (Metrohm) standardized by NBS buffers. The change in the pH during equilibration,  $\Delta\text{pH}$ , was then determined  $\{\Delta\text{pH} = \text{pH}(\text{blank solution}) - \text{pH}(\text{suspension})\}$ . The pzc was identified as the pH where the minimum  $\Delta\text{pH}$  value was obtained.

**Microelectrophoresis.** The  $\zeta$  potential of the solid particles was measured using a Zetasizer 5000 (Malvern Instruments Ltd.) microelectrophoresis apparatus at constant temperature, 25 °C. Sufficiently dilute suspensions of a given oxide were prepared with constant ionic strength, 0.01 M. The pH of the suspensions was adjusted by small additions of a 1 M  $\text{HNO}_3$  or KOH solution.

**Development of a Simulation Procedure for the PMT Technique.** To develop a simulation procedure for the PMT technique, we have to consider a hypothetical suspension that is going to be titrated. The suspension has two basic components: the electrolyte solution and the solid metal (hydr)oxide. To describe completely the interfacial region between these two components, we have to select a surface-charging mechanism for the oxide and an electrostatic model for the electric double layer developed between the surface of the solid particles and the electrolytic solution. Moreover, values of several parameters related to the hypothetical metal (hydr)oxide, such as the surface site density and specific area, should also be assumed.

Table 1 presents the entire surface-charging models and the electrostatic models that were adopted as well as the parameters necessary to perform the simulation procedure.

In this point it should be noticed that we have assumed a uniform potential developing around the particle surface. This potential corresponds to a homogeneous surface or to a heterogeneous surface with a random distribution of the various surface sites.<sup>31</sup> This is the most common approach because the assumption of a patchwise heterogeneous surface (e.g., a mixture of different particles or particles with large crystal planes) is more complicated to study and is difficult to test experimentally. However, our group is performing work now to study this case to investigate whether the PMT technique can be used in more complex situations to gain more insight.

**First Step of the Simulation Procedure: Calculation of the Total Number of Surface  $\text{H}^+$  Ions before Impregnation.** In the first step of the simulation procedure, it is necessary to input into the program two important parameters: (i) the initial quantity of base added to the suspension to reach the initial pH of the titration procedure for the system and (ii) the initial total concentration of the hydrogen ions,  $[\text{H}^+]_{\text{t, in}}$ , present in the suspension.

The first quantity is easily determined when the volume,  $V_{\text{base}}$ , and the concentration of the added base,  $C_{\text{base}}$  are known. The hypothetical values used in our simulation procedure are equal to 0.2 mL and 1 M, respectively.

The calculation of  $[\text{H}^+]_{\text{t, in}}$  depends on the surface-charging model adopted. To be specific, concerning the 1 site/1 pK model,<sup>32–34</sup> the calculation is based on equilibrium 1. (Equilibria 1–6 are compiled in Table 1.) Assuming that the surface charge of the hydr(oxide) before impregnation is equal to zero, we may write that  $[\text{SOH}_2^{+1/2}] = [\text{SOH}^{-1/2}] = N_s/2$ . Taking into account that only the second protons involved in the  $[\text{SOH}_2^{+1/2}]$  groups participate in the aforementioned equilibrium, we may write that

$$[\text{H}^+]_{\text{t, in}} = [\text{SOH}_2^{+1/2}] = \frac{N_s}{2} \quad (1 \text{ site/1 pK model}) \quad (7)$$

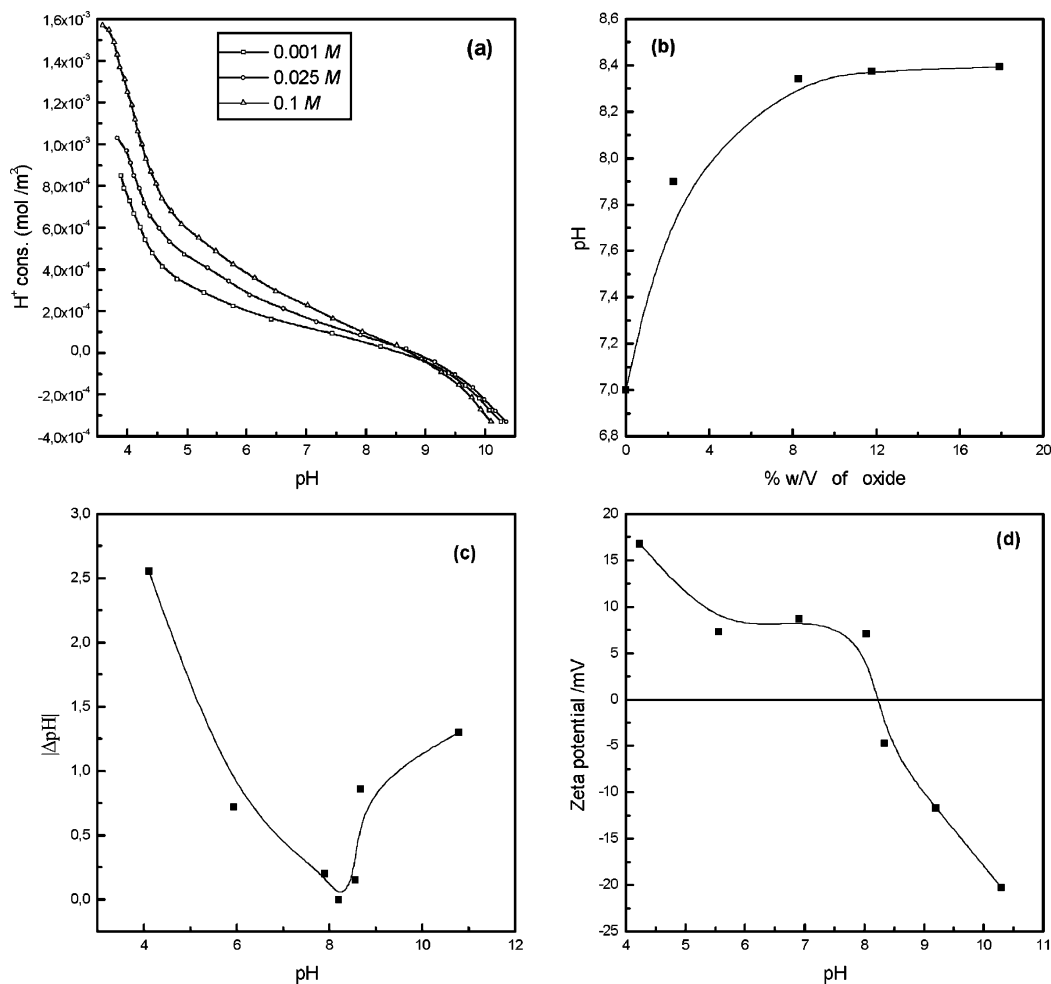


**Figure 2.** Experimental curves corresponding to the techniques widely used for the determination of the pzc of  $\gamma$ - $\text{Al}_2\text{O}_3$ : (a) potentiometric titrations, (b) mass titrations, (c) immersion technique, (d) microelectrophoresis.

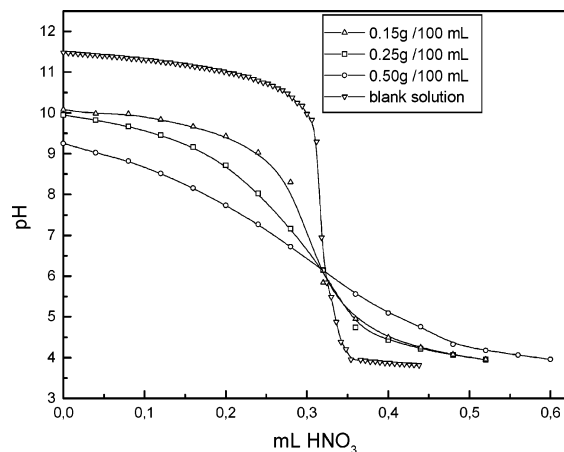


**Figure 3.** Experimental curves corresponding to the proposed potentiometric mass titrations technique for the determination of the pzc of  $\text{TiO}_2$ .

Concerning the 1 site/2 pK model,<sup>35–37</sup> described by equilibria 2 and 3, the neutrality of the surface before impregnation results in  $[\text{SO}^-] = [\text{SOH}_2^+]$ . Therefore, the value of  $[\text{H}_{\text{t, in}}^+]$  is given by

$$[\text{H}_{\text{t, in}}^+] = [\text{SOH}] = N_s \quad (1 \text{ site}/2 \text{ pK model}) \quad (8)$$

In the case of the Music model,<sup>38–40</sup> the determination of  $[\text{H}_{\text{t, in}}^+]$  is more complicated. It depends on the number of equilibria (4) and the nature of surface hydroxyls. The computer

program performs the calculation of  $[\text{H}_{\text{t, in}}^+]$  once the equilibria (4) and the electrostatic model have been defined (Table 1). The calculation is based on the following general equation:

$$[\text{H}_{\text{t, in}}^+] = \sum [\text{S}_i \text{H}^{z_i+1}] \quad (\text{multisite model}) \quad (9)$$

*Second Step of the Simulation Procedure: Calculation of the Equilibrium pH of the Suspension.* Having determined the two above-mentioned parameters (initial amount of added base and total number of hydrogen ions), we can proceed to the second step of the simulation procedure. In this step, we consider the combination of a surface-charging model and an electrostatic model (Table 1), and we also introduce into the program the above-calculated parameters as well as the values for the parameters illustrated in the third column of Table 1, relative to a given combination of surface charging with an electrostatic model.

At this point, it should be noted that the pzc value of the hypothetical hydr(oxide) is determined once the pK values (for the 1site/1pK and 1site/2pK models) and the  $pK_i$ ,  $z_i$ , and  $Ns_i$  values (for the Music model) have been selected.

The output, in this step, is the equilibrium pH of the suspension. We call this  $\text{pH}_{\text{init}}$  because this will be the initial pH of the titration procedure, which is the next step. The  $\text{pH}_{\text{init}}$  calculation is repeated several times for different values of the hydr(oxide) mass added in the suspension.

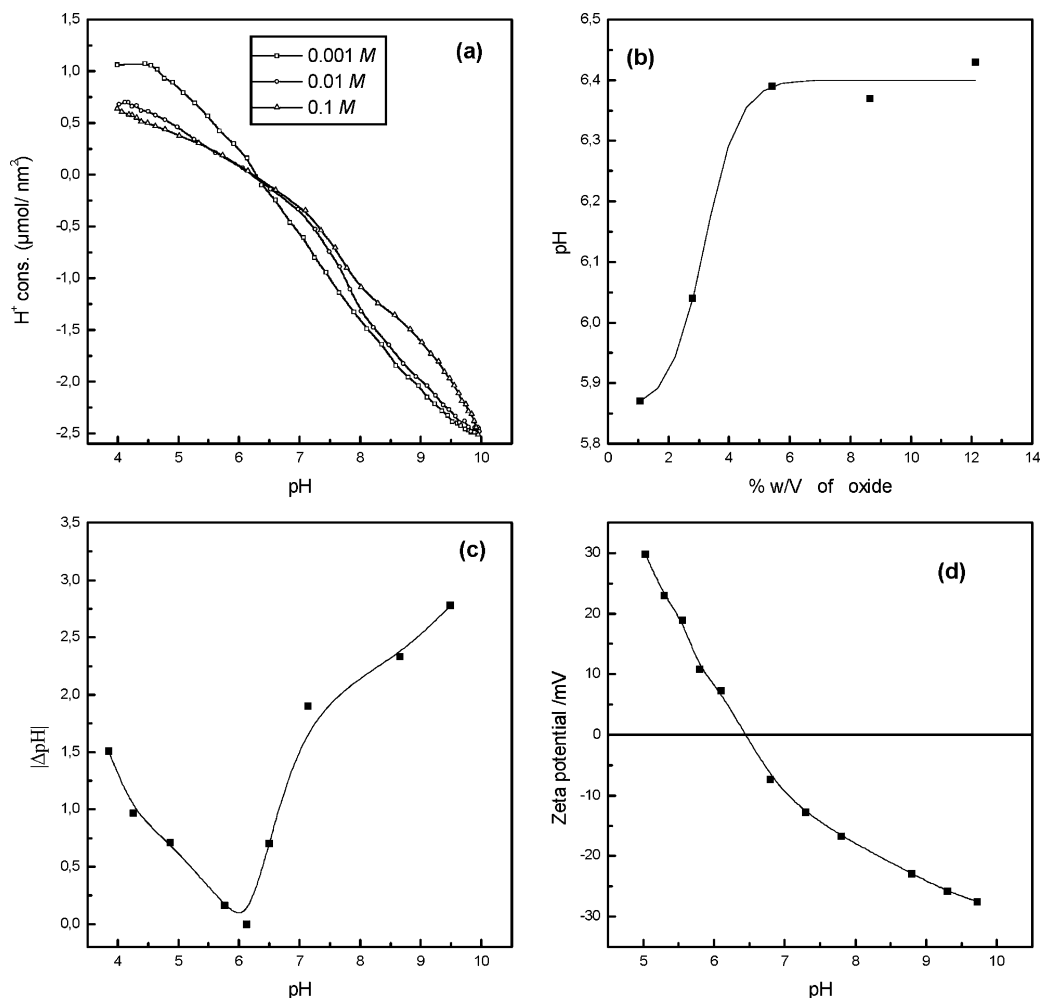


**Figure 4.** Experimental curves corresponding to the techniques widely used for the determination of the pzc of  $\text{TiO}_2$ : (a) potentiometric titrations, (b) mass titrations, (c) immersion technique, (d) microelectrophoresis.

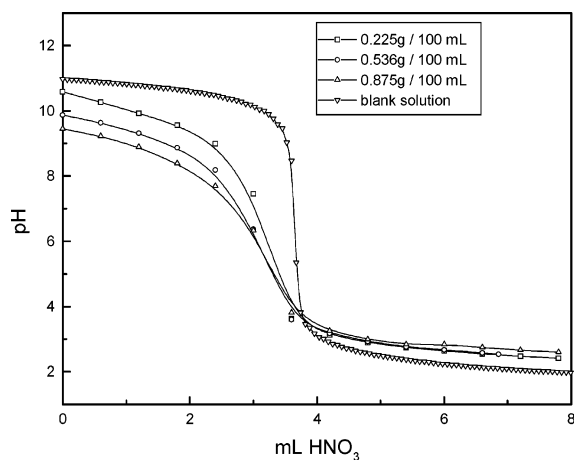


**Figure 5.** Experimental curves corresponding to the proposed potentiometric mass titrations technique for the determination of the pzc of  $\text{SiO}_2$ .

**Third Step of the Simulation Procedure: Potentiometric Mass Titrations.** In the third step of the procedure, we derive the potentiometric mass titration curves. Each time, the program uses a given combination of models selected in the previous step for calculating the volume of the added acid in the suspension, ( $V_{\text{added}}$ ), versus the final pH of the suspension after each addition. The initial pH,  $\text{pH}_{\text{init}}$ , of the titration curve is that calculated in the previous step. The determination of  $V_{\text{added}}$

at each pH value of the suspension is based on the following equation:

$$[V_{\text{added}}] = \frac{[\text{H}_{\text{sol}}^+] + [\text{H}_{\text{surf}}^+] + [\text{H}_{\text{H}_2\text{O}}^+]}{C_{\text{acid}}} V_{\text{susp}} \quad (10)$$

where  $V_{\text{susp}}$  and  $C_{\text{acid}}$  represent the volume of the suspension and the concentration of the added acid, whereas by  $[\text{H}_{\text{sol}}^+]$ ,  $[\text{H}_{\text{surf}}^+]$ ,  $[\text{H}_{\text{H}_2\text{O}}^+]$  we denote the concentration of  $\text{H}^+$  ions accumulated in the solution, consumed by the surface hydroxyls and by the hydroxyl ions of the solution, respectively. The calculation is performed by transforming eq 10 into the following equation:

$$\begin{aligned} [V_{\text{added}}] &= \frac{[\text{H}_{\text{sol}}^+] + [\text{H}_{\text{surf}}^+] + [\text{H}_{\text{H}_2\text{O}}^+]}{C_{\text{acid}}} V_{\text{susp}} \\ &= \{[\text{H}_{\text{sol},f}^+] - [\text{H}_{\text{sol},in}^+] + [\text{H}_{\text{surf},f}^+] - [\text{H}_{\text{surf},in}^+] + \\ &\quad [\text{OH}_{\text{sol},in}^-] - [\text{OH}_{\text{sol},f}^-]\} V_{\text{susp}} C_{\text{acid}} \quad (11) \end{aligned}$$

In the above equation, subscripts “in” and “f” denote, respectively, the initial (calculated at the second step) and final (after each addition of acid) concentrations.

The calculation of  $V_{\text{added}}$  versus pH curves is repeated several times for different values of the hydr(oxide) mass immersed in the suspension.



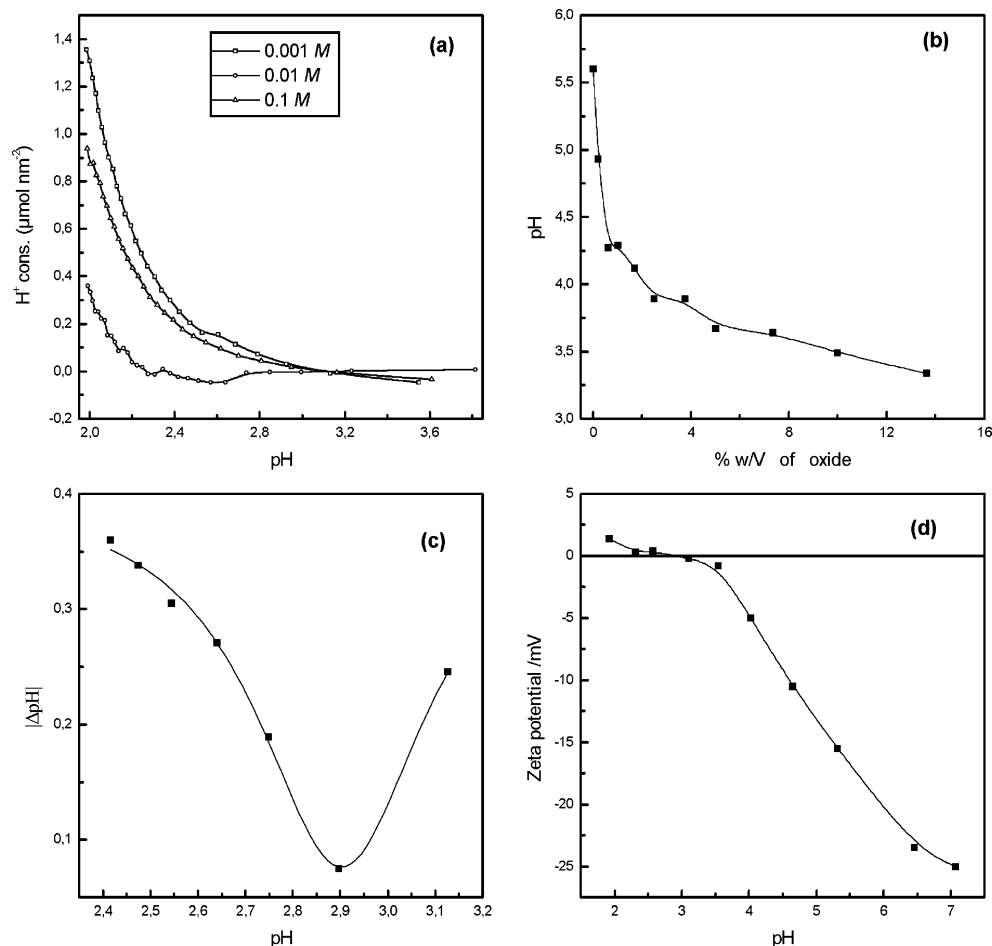


**Figure 6.** Experimental curves corresponding to the techniques widely used for the determination of the pzc of  $\text{SiO}_2$ : (a) potentiometric titrations, (b) mass titrations, (c) immersion technique, (d) microelectrophoresis.

Finally, it should be noted that all of the above calculations were carried out with ECOSAT, a computer code for the calculation of chemical equilibria.<sup>41</sup>

## Results and Discussion

**Experimental Titration Curves.** The experimental curves corresponding to the novel PMT technique, recorded for  $\gamma\text{-Al}_2\text{O}_3$ , are illustrated in Figure 1 whereas the experimental curves recorded for the same oxide, which correspond to the traditional PT, MT, IT, and (ME) techniques, are illustrated in Figure 2. It may be seen that all techniques provide a pzc (iep) value in the range of 8.0–8.6 (Table 2) in accordance with the literature.<sup>4,26,42</sup> A careful inspection of these curves shows that the pzc is more clearly identified using the PMT technique, even with its quick-scan version. In contrast to that, it may be seen that the usually applied PT technique provides a pzc value with the maximum deviation from the mean value. Moreover, this technique provides a triangle rather than a common intersection point.

The experimental curves corresponding to the PMT technique, recorded for  $\text{TiO}_2$ , are illustrated in Figure 3 whereas the experimental curves recorded for the same oxide, which correspond to the traditional methodologies, are depicted in Figure 4. For this oxide, all techniques, including the quick-scan version of PMT, result in a quite accurate determination of the pzc (iep) in the range of 6.0–6.4 (Table 2), in accordance with the literature.<sup>4,26,42–44</sup>

The determination of pzc (iep) for  $\text{SiO}_2$  using the PMT and the techniques mentioned above is illustrated in Figures 5 and

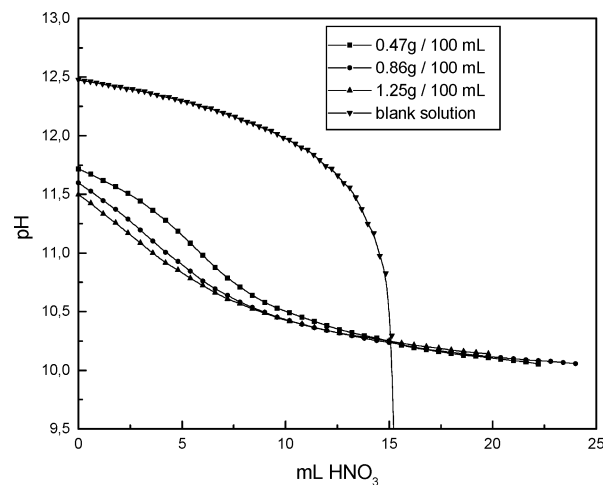


**Figure 7.** Experimental curves corresponding to the proposed potentiometric mass titrations technique for the determination of the pzc of  $\text{MgO}$ .

6, respectively. You may observe that the PMT, PT, IT, and ME techniques provide a pzc (iep) value in the range of 2.9–3.2, in agreement with the literature.<sup>4,26,42</sup> In contrast, using the MT technique, one cannot reach the pzc value because the quite high  $\text{SiO}_2$  concentration required and the very low pzc value cause the gelation of the suspension. Therefore, using MT, the pzc is estimated to be in the range of 3.2–3.5. In this case, the weakness of the MT technique is rather obvious. At this point, it should be mentioned that quite recently an improved alternative to the MT technique that overcomes the aforementioned

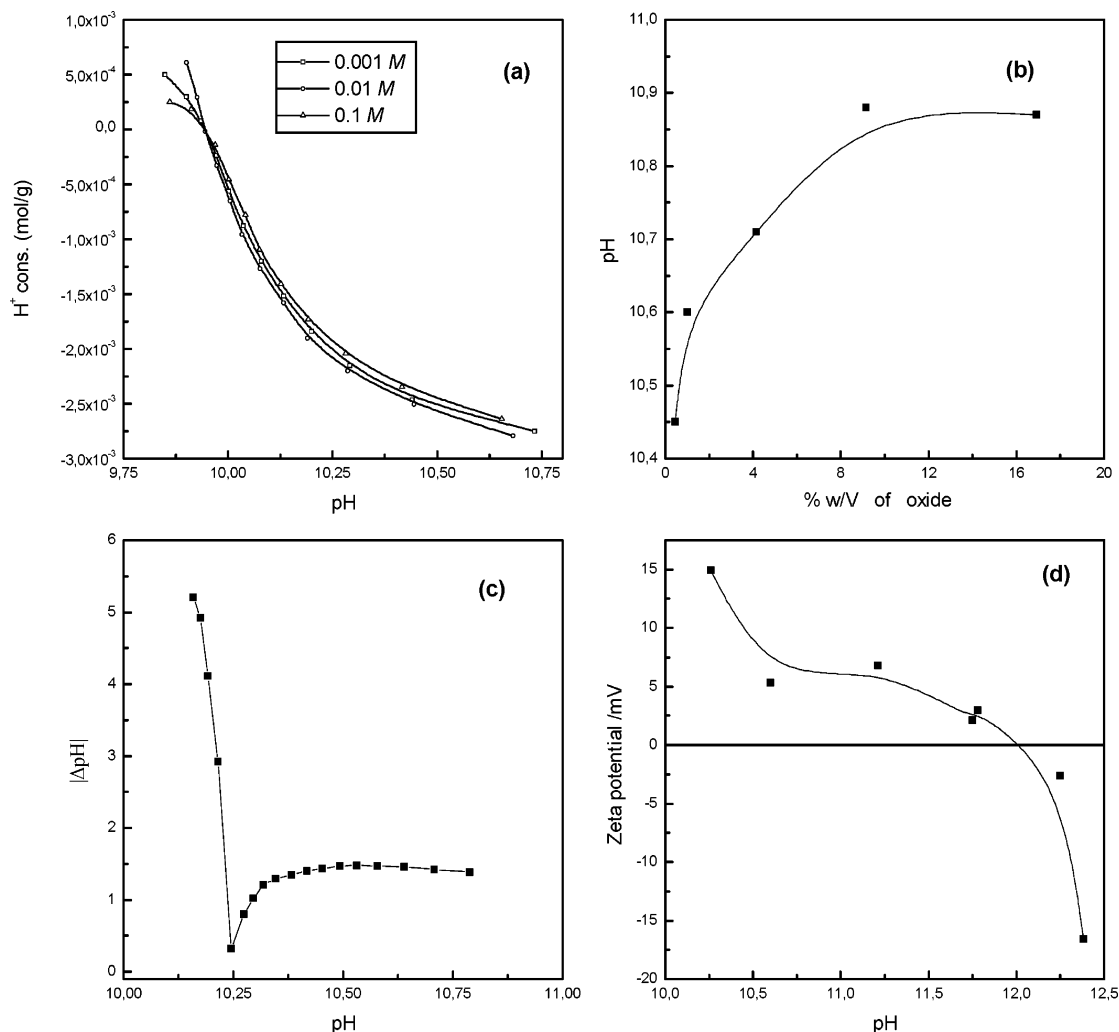


**Figure 8.** Experimental curves corresponding to the techniques widely used for the determination of the pzc of MgO: (a) potentiometric titrations, (b) mass titrations, (c) immersion technique, (d) microelectrophoresis.

weakness has been developed by Park and Regalbuto.<sup>45</sup> However, the application of this technique requires a special pH meter setup with a short electrode life.

Moreover, a careful inspection of Figure 5 shows that at pH values lower than 4 the titration curves' convergence renders unclear the CIP. Thus, it is obvious that the PMT technique in its original form presents a weakness in cases where the pzc is located at pH values lower than a critical value. This point will be elucidated in the following section, where the simulation results will be discussed.

Finally, the experimental curves used for the determination of the pzc (iep) of MgO, corresponding to the PMT and the traditionally used techniques, respectively, are illustrated in Figures 7 and 8. One may observe that all techniques, with the exception of MT, provide pzc values in the range of 10.0–10.3 whereas the MT provides a somewhat greater value (10.9). Moreover, the ME technique results in an iep value of 12. These differences in the values of the pzc (which can also be found in the literature<sup>4,23,26,46,47</sup>) could be attributed to the increased dissolution of MgO as the pH decreases or to a possible specific adsorption of cations ( $K^+$ ,  $Mg^{2+}$ ) on the MgO–electrolyte solution interface.

A careful observation of Figure 7 shows that at pH values lower than 10.5 the PMT curves of the suspensions cannot be distinguished. Therefore, in this case, the pzc is identified as the CIP of the titration curve of the blank solution with the corresponding curve of one of the three suspensions. However,

a plausible question is raised at this point. Is the fact that the titration curves of the suspensions cannot be distinguished in the pH range of 10.5–9.5 due to the well known remarkable dissolution of MgO,<sup>48</sup> or is it due to an intrinsic weakness of the PMT technique? The simulation results will be used to answer this question.

In conclusion, the results described above clearly demonstrate that the novel PMT technique, principally, its quick-scan version, may be used for a rapid and accurate determination of the pzc at least for oxides immersed in electrolyte solutions.

**Simulation Curves.** As already mentioned in the Introduction, the most important goal in the present work is to demonstrate *quantitatively* that the application of the PMT technique indeed provides pzc values. The simulation curves illustrated in Figures 9a–c show that the PMT technique in its original form (pH vs  $V_{\text{added acid}}$ ) actually results in the pzc values initially assumed for the model oxide, at least in the pH range of 10.5–6.0, and for the model combination (1 site/1 pK, DDL<sup>49</sup> model) related to the minimum number of model parameters (Ns, SC, SSA, pK, and  $I$ ). However, the simulation curves illustrated in Figure 9d show that the PMT technique in its original form fails to determine clearly a pzc value located at relatively low pH. Thus, in the case of  $SiO_2$  (Figure 5), we observe an intrinsic weakness in the original form of the PMT at low pH values. In contrast to the above, it may be seen that the initially assumed pzc value for the model oxide is actually achieved by the PMT simulation curves provided that the

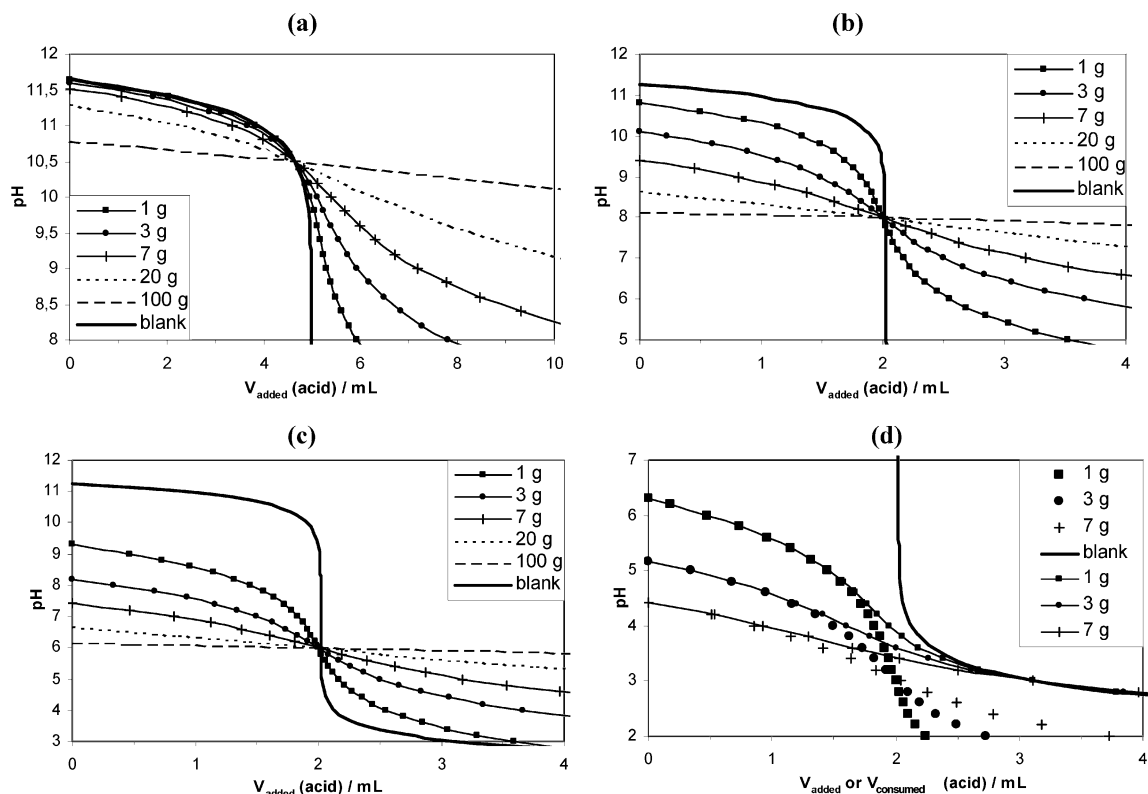


**Figure 9.** Potentiometric mass titration curves derived from simulation using the 1 site/1 p*K* and DDL models and the following data: (a) |p*K*| = 10.5, (b) |p*K*| = 8.0, (c) |p*K*| = 6.0, (d) |p*K*| = 3.0. Large symbols in d correspond to  $V_{\text{consumed}}$  values, and lines with small symbols correspond to  $V_{\text{added}}$  values.

volume of the added acid ( $V_{\text{added}}$ ) on the horizontal axis is replaced by the volume of the acid consumed ( $V_{\text{consumed}}$ ) by the suspension. It is obvious that in this case one cannot use the titration curve of the blank solution.

To investigate this point further, we compare eq 11 used for determining  $V_{\text{added}}$  with the following expression used for determining  $V_{\text{consumed}}$ :

$$[V_{\text{consumed}}] = \frac{[\text{H}_{\text{surf}}^+] + [\text{H}_{\text{H}_2\text{O}}^+]}{C_{\text{acid}}} V_{\text{susp}}$$

$$= \frac{[\text{H}_{\text{surf,f}}^+] - [\text{H}_{\text{surf,in}}^+] + [\text{OH}_{\text{sol,in}}^-] - [\text{OH}_{\text{sol,f}}^-]}{C_{\text{acid}}} V_{\text{susp}} \quad (12)$$

It may be seen that, although these expressions are generally different, above a critical pH value the term  $[\text{H}_{\text{sol,f}}^+] - [\text{H}_{\text{sol,in}}^+]$  is negligible and eq 11 is reduced to eq 12. To determine this critical pH value, we calculated both  $V_{\text{added}}$  and  $V_{\text{consumed}}$  over the whole pH range. Figure 10 shows that the  $V_{\text{consumed}}$  values are identical to the corresponding  $V_{\text{added}}$  values above pH 4. Thus, above this value, both the  $V_{\text{added}}$  and  $V_{\text{consumed}}$  values may be used to construct the PMT curves and determine the pzc. Obviously, using the  $V_{\text{added}}$  values, one would apply the quick-scan alternative of the PMT mentioned in the Introduction by recording only two potentiometric curves—one for the blank solution and one for a suspension of a given amount of the immersed oxide. In contrast, for pH values lower than 4, the experimental pH versus  $V_{\text{consumed}}$  (acid) PMT curves must be constructed for an accurate determination of the pzc.

Returning to Figure 9a, we may observe that for pH values higher than the pzc (10.5–11.5) large amounts of the immersed oxide are required for the titration curves to be clearly

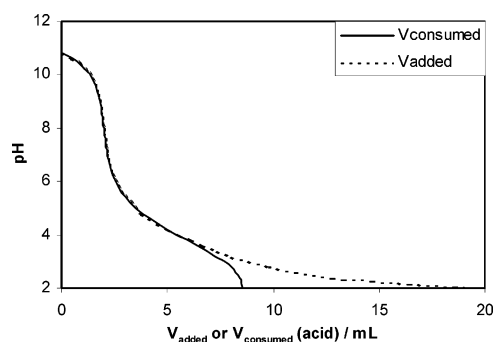


**Figure 10.** Comparison of the variation in  $V_{\text{added}}$  and  $V_{\text{consumed}}$  with pH as determined using eqs 11 and 12, respectively.

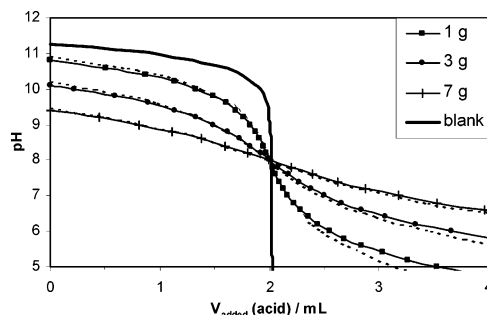


**Figure 11.** Potentiometric mass titration curves derived from simulation using the 1 site/1 p*K* and DDL models and |p*K*| = 8.0. Dotted (solid) lines have been calculated using  $N_s = 3$  (8) sites  $\text{nm}^{-2}$ .

distinguished. This is rather expected because the |p*K*| value and thus the pzc of this model oxide are too high. However, even in this case, the application of PMT in its original form provides a clear CIP because at pH values just below CIP the titration curves are easily distinguished. The fact that the titration curves are distinguishable in the pH range of 10.5–9.5 clearly



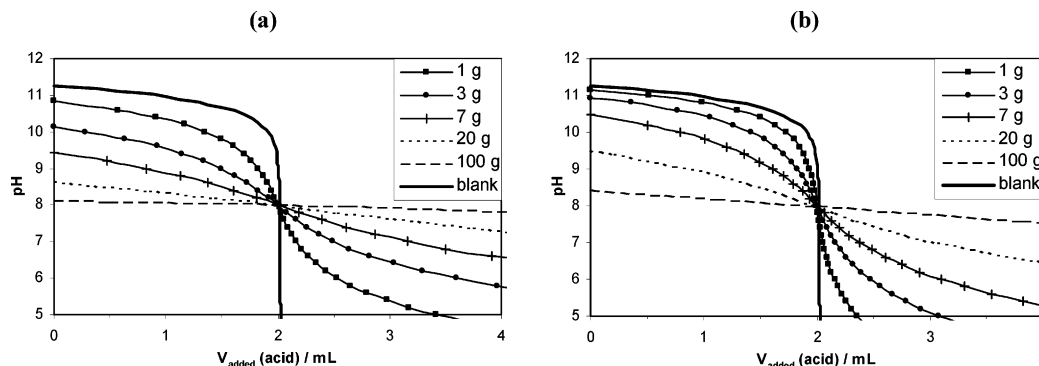


**Figure 12.** Potentiometric mass titration curves derived from simulation using the 1 site/2 pK and DDL models and the following data:  $pzc = 8.0$ , (a)  $|\Delta pK| = 2.0$ , (b)  $|\Delta pK| = 6.0$ .

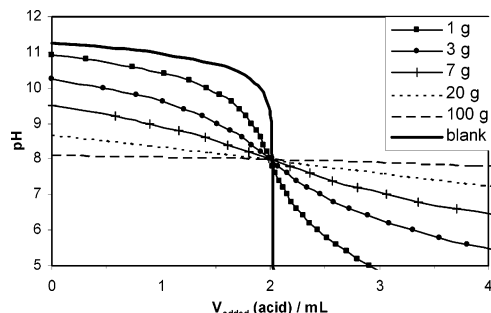


**Figure 13.** Potentiometric mass titration curves derived from simulation using the Music and DDL models with the parameters given in Table 3.

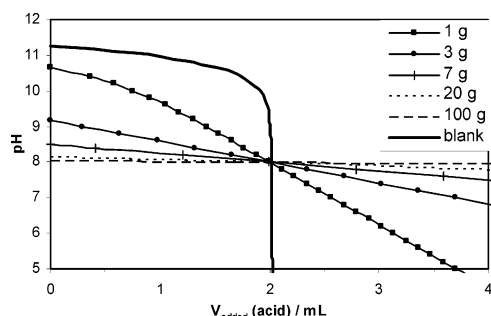


**Figure 14.** Potentiometric mass titration curves derived from simulation using the 1 site/1 pK and CC models and  $|pK| = 8.0$ .

shows that the convergence of these curves, observed in the case of MgO in this pH range, does not reflect an intrinsic weakness of the PMT technique but is due to the well known surface dissolution of this oxide in this pH range.

Taking into account the underlying idea on which the PMT technique has been based, one might argue that for a given amount of the immersed oxide the deviation of the pH value achieved for the suspension from the corresponding one achieved for the blank solution, for a given value of the  $V_{\text{added}}$  or  $V_{\text{consumed}}$ , should be proportional to the surface site density. In contrast to the above, Figure 11 clearly shows that the drastic change in the surface site density from 3 sites  $\text{nm}^{-2}$  (dot lines) to 8 sites  $\text{nm}^{-2}$  (solid lines) does not bring about any remarkable effect on the aforementioned deviation in pH. This (rather unexpected from a first view) result reflects the extremely important role of the electrically charged surface and thus of the double layer developed between the oxide surface and the bulk solution that unfortunately has been underestimated in several adsorption studies. To be specific, the increase of the mass of the immersed oxide increases the adsorption–desorption sites of the suspension without affecting the surface charge density or surface potential and thus the distribution of the  $\text{H}^+$

ions in the double layer on going from the surface to the bulk solution. In contrast to that, the increase in the value of the site density increases the number of adsorption–desorption sites of the surface, but at the same time, it causes an increase in the surface charge density and in the surface potential. Thus, at relatively high (low) pH values where the surface is negatively (positively) charged, the increase in the number of sites releasing (receiving) protons is compensated by the increase in the negative (positive) surface potential, which in turn inhibits the desorption (adsorption) of the  $\text{H}^+$  ions. The above are quantitatively expressed by the well-known Boltzmann equation,

$$[\text{H}_{\text{surface}}^+] = [\text{H}_{\text{bulk}}^+] \exp\left(-\frac{F\Psi_0}{RT}\right) \quad (13)$$

which illustrates the relationship of the concentration of  $\text{H}^+$  ions in the bulk solution,  $[\text{H}_{\text{bulk}}^+]$ , used to determine the pH, with the value of the surface potential,  $\Psi_0$ , and the value of the surface concentration of  $\text{H}^+$  ions,  $[\text{H}_{\text{surface}}^+]$ .

The above-explained insensitivity of the titration curves from the surface site density,  $N_s$ , has been also reported in the past (e.g. refs 5 and 50). Hayes et al.<sup>50</sup> have performed a systematic calculation of the influence of the value of  $N_s$ , as well as of other double-layer parameters, on the titration curves (pH vs  $V_{\text{added}}$  acid). They have found that all double-layer models are relatively insensitive to changes in the value of  $N_s$ , provided that this value is in the range of values that are reasonable for mineral oxides (2–20 sites  $\text{nm}^{-2}$ ).

Up to this point, we have *quantitatively* demonstrated that the application of the PMT technique results in the determination of the pzc values over the whole pH range, provided that the very simple 1 site/1 pK model describes the surface charging of the model oxide. Although this homogeneous model has been used several times in the past to model  $\text{H}^+$  adsorption (e.g., refs 32–34, 51, and 52), the more general, also homogeneous 1 site/ 2pK model has also been used extensively in the past (e.g., refs 35–37, 42, 50, 53, and 54). It is therefore interesting to investigate whether the PMT technique indeed gives pzc values in cases where the surface charging is described by the 1 site/2 pK model. To do this, we have simulated the PMT technique assuming two pairs of pK values for the model oxide:  $|pK_1| = 9$ ,  $|pK_2| = 7$  and  $pK_1 = 11$ ,  $pK_2 = 5$ , both resulting in the same pzc value ( $pzc = 8$ ) but at two different  $\Delta pK$  values,  $|\Delta pK| = 2$  and 6, respectively.

The potentiometric titration curves derived by the simulation procedure are presented in Figure 12a and b. An inspection of these Figures clearly shows that the PMT technique may be used to determine the pzc in cases where the 1 site/2 pK model describes the charging-surface oxide mechanism. A comparison

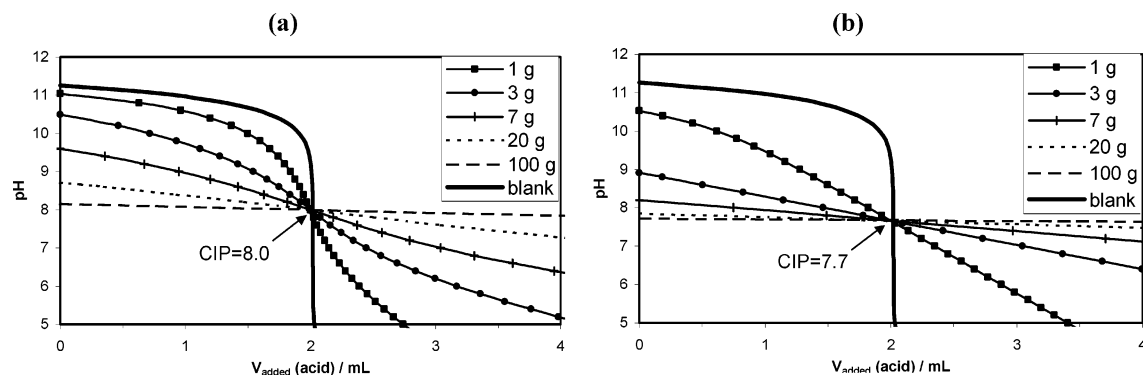


**Figure 15.** Potentiometric mass titration curves derived from simulation using the 1 site/1 pK and BS models and the following data:  $|pK| = 8.0$ , (a)  $pK_C = pK_A = 1.0$ ,  $I = 0.01$  M  $KNO_3$ , (b)  $pK_C = 0.3$ ,  $pK_A = 1.2$ ,  $I = 1$  M  $KNO_3$ .

**TABLE 3: Set of Surface Sites Considered for the Model Metal (Hydr)oxide According to the Music Model**

equation	parameters	values
$S_1^{-0.75} + H^+ \xrightleftharpoons{K_1} S_1H^{+0.25}$ (14)	$pK_1, Ns_1$	$-10.5, 1.5 \text{ sites nm}^{-2}$
$S_2^{-0.50} + H^+ \xrightleftharpoons{K_2} S_2H^{+0.50}$ (15)	$pK_2, Ns_2$	$-8.65, 3.0 \text{ sites nm}^{-2}$
$S_3^{-0.25} + H^+ \xrightleftharpoons{K_3} S_3H^{+0.75}$ (16)	$pK_3, Ns_3$	$-6.5, 1.5 \text{ sites nm}^{-2}$
$S_4^{-0.50} + H^+ \xrightleftharpoons{K_4} S_4H^{+0.50}$ (17)	$pK_4, Ns_4$	$-4.0, 2.0 \text{ sites nm}^{-2}$

of parts a and b of Figure 12 shows that although the selection of two different pairs of the pK values corresponding to two different  $\Delta pK$  values induces the derivation of two different sets of titration curves, both sets of curves intersect at the same pH value corresponding to the initially assumed pzc for this model oxide.

From the beginning of the previous decade, a trend toward the application of the heterogeneous multisite model (Music model), developed by Hiemstra et al, for modeling the acid–base behavior of a (hydr)oxide immersed in electrolytic solution<sup>38–40</sup> was observed. To examine the generality of the PMT technique, it seems reasonable to us to investigate whether this methodology results in pzc values even in cases where the charging mechanism of an oxide surface is described by the heterogeneous Music model. To do this, we have simulated the PMT technique using a hypothetical oxide described by equilibria 14 and 15 and the  $pK_i$  and  $Ns_i$  constants involved in Table 3. An inspection of Figure 13 clearly shows that the PMT technique may be also applied to the determination of pzc values even in cases where on the metal oxide surface various kinds of sites are developed for the adsorption–desorption of  $H^+$  ions.

The simulations of the PMT technique presented so far were based on the assumption that the double layer developed between the oxide surface and the bulk solution is described by the diffuse double layer model.<sup>49</sup> Finally, to accomplish our research on the impact of the proposed PMT technique, we investigated whether this methodology actually results in pzc values in cases where different interfacial models, such as the well known constant capacitance<sup>55,56</sup> or basic Stern<sup>38,57,58</sup> model, are more appropriate to the description of the interfacial region. To reduce the number of adjustable parameters, each of the above models has been combined with the simple 1 site/1 pK model.

A comparison of Figure 9b with Figures 14 and 15a shows that although the change in the double-layer model affects the

titration curves derived by applying the simulation procedure, it does not affect the position of the CIP and the pzc value determined by PMT. However, a comparison of parts a and b of Figure 15 shows that when the basic Stern model describes the interfacial region the PMT technique provides the correct pzc value only in the case where the constants related to the formation of ion pairs are equal ( $pK_C = pK_A$ ). On the contrary, a slight shift in CIP should be expected when  $pK_C \neq pK_A$ .<sup>43,59</sup> This shift becomes significant as the ionic strength increases (Figure 15b) and is in agreement with the corresponding (reverse) shift of the iep, which has been reported in the literature for various hydr(oxides).<sup>43,60–63</sup>

To be more specific, let us consider the case when  $pK_C < pK_A$  (namely, a stronger affinity of cations than that of anions). The combination of a relatively large difference in the values of  $pK_C$  and  $pK_A$  with high ionic strength causes an increase in the concentration of ion pairs in equilibrium 5 and consequently an accumulation of positive charge in the Stern layer. The blocking of  $SOH^{-1/2}$  surface groups by the cations of the electrolyte (equilibrium 5) shifts equilibrium 1 to the left, rendering the surface of the (hydr)oxide more negative. Thus, to neutralize the surface (reach the pzc), a lower pH value is necessary because it is compared with the situation where ion pair formation is negligible or the constants related to the formation of ion pairs are equal ( $pK_C = pK_A$ ). For this reason, the CIP is observed at a lower pH value (Figure 15b). An opposite shift of the CIP is observed in the case where  $pK_C > pK_A$  (namely, a stronger affinity of anions than of cations). For more insight, Sposito<sup>2</sup> has given an interesting analysis of this phenomenon in terms of charge densities of the various layers of the interfacial region.

The above explains the ionic strength dependence of the pzc and suggest that when an accurate pzc value has to be determined by PMT it is better to confirm it by the use of two different background electrolytes with concentration up to 0.1 M. At this point, it is worth noting that in cases when  $pK_A \neq pK_C$  the traditional PT technique provides a triangle instead of a CIP, thus resulting in the determination of a pzc value with relatively low accuracy. Finally, it should be noted that like all other methods the CIP obtained by the PMT technique could be affected by contaminating the sample with ions that are strongly bound to the surface of the (hydr)oxide.

## Concluding Remarks

The most important results drawn from this work may be summarized as follows:

(1) It was *quantitatively* demonstrated that the application of the quick-scan version of the PMT technique realized by recording the titration curve of the blank solution (pH vs  $V_{added}$

acid) and the corresponding curve of a suspension of a given amount of the immersed oxide results in the determination of the pzc provided that its value is located above pH 4.

(2) It was, moreover, *quantitatively* demonstrated that the application of the "typical" version of PMT realized by recording the titration curves of three different suspensions (pH vs  $V_{\text{consumed}}$  acid) containing different masses of the immersed oxide provides the pzc value of this oxide over the whole pH range.

(3) It was demonstrated that the pzc determined using PMT does not depend on the charging mechanism of the oxide surface (1 site/1 pK, 1 site/2 pK, multisite model) or on the structure of the double layer (diffuse layer, constant capacitance, basic Stern model).

(4) When the interface is described by the basic Stern model, the pzc value determined using PMT deviates slightly from the true value in cases where the value of the constant related to the formation of ion pairs of the positive counterions is different from the corresponding value of the negative counterions.

(5) It was theoretically confirmed that the change in the surface site density does not actually affect the titration curves.

## References and Notes

- (1) Vakros, J.; Kordulis, Ch.; Lycourghiotis, A. *Chem. Commun.* **2002**, 17, 1980.
- (2) Sposito, G. *Environ. Sci. Technol.* **1998**, 32, 2815.
- (3) Eggleston, C. M.; Jordan, G. *Geochim. Cosmochim. Acta* **1998**, 62, 1919.
- (4) Kosmulski, M. *J. Colloid Interface Sci.* **2002**, 253, 77.
- (5) Hiemstra, T.; Van Riemsdijk, W. H. *J. Colloid Interface Sci.* **1996**, 179, 488.
- (6) Sverjensky, D. A.; Sahai, N. *Geochim. Cosmochim. Acta* **1996**, 60, 3773.
- (7) Dzombak, D. A.; Morel, F. M. M. *Surface Complexation Modeling: Hydrous Ferric Oxide*; Wiley: New York, 1990.
- (8) Bolt, G. H.; Van Riemsdijk, W. H. *Soil Chemistry B: Physico-chemical Models*; Bolt, G. H., Ed.; Elsevier: Amsterdam, 1982.
- (9) Sposito, G. *The Surface Chemistry of Soils*; Oxford University Press: New York, 1984.
- (10) Barrow, N. J. *Reactions with Variable Charge Soils*; Nijhoff: Dordrecht, The Netherlands, 1987.
- (11) Davis, J. A.; Kent, D. B. In *Mineral-Water Interface Geochemistry: Reviews in Mineralogy*; Hochella, M. F., White, A. F., Eds.; Mineralogical Society of America: Washington, DC, 1990; Vol. 23, p 177.
- (12) Brunelle, J. P. *Pure Appl. Chem.* **1978**, 50, 1211.
- (13) Wang, L.; Hall, K. W. H. *J. Catal.* **1982**, 77, 232.
- (14) Lycourghiotis, A. *Preparation of Catalysts VI*; Poncelet, G., Martens, J., Delmon, B., Jacobs, P. A., Grange, P., Eds.; Elsevier: Amsterdam, 1995; p 95.
- (15) Schwarz, J. A.; Contescu, C.; Contescu, A. *Chem. Rev.* **1995**, 95, 477.
- (16) Lambert, J.-F.; Che, M. *J. Mol. Catal. A* **2000**, 162, 5.
- (17) Bourikas, K.; Hiemstra, T.; Van Riemsdijk, W. H. *J. Phys. Chem. B* **2001**, 105, 2393.
- (18) Vakros, J.; Bourikas, K.; Kordulis, Ch.; Lycourghiotis, A. *J. Phys. Chem. B* **2003**, 107, 1804.
- (19) Deo, G.; Wachs, I. E. *J. Phys. Chem.* **1991**, 95, 5889.
- (20) Spieker, W. A.; Regalbuto, J. R. *Chem. Eng. Sci.* **2001**, 56, 3491.
- (21) Carrier, X.; Lambert, J. F.; Che, M. *J. Am. Chem. Soc.* **1997**, 119, 10137.
- (22) Noh, J.; Schwarz, J. *J. Colloid Interface Sci.* **1989**, 130, 157.
- (23) Lyklema, J. *Adsorption from Solution at the Solid/Liquid Interface*; Parfitt, G. D., Rochester, C. H., Eds.; Academic Press: New York, 1983; Chapter 5.
- (24) Tewari, P.; Campbell, A. *J. Colloid Interface Sci.* **1982**, 55, 531.
- (25) Berube, Y. G.; De Bruyn, P. L. *J. Colloid Interface Sci.* **1968**, 27, 305.
- (26) Parks, G. *Chem. Rev.* **1965**, 65, 177.
- (27) Lyklema, J. *Solid/Liquid Dispersions*; Thadros, Th. F., Ed.; Academic Press: London, 1987; Chapter 3.
- (28) Lyklema, J. *Fundamentals of Interface and Colloid Science*; Academic Press: London, 1995; Chapter 3.
- (29) Sonnefeld, J. *Colloids Surf., A* **2001**, 190, 179.
- (30) Lycourghiotis, A. *Acidity and Basicity of Solids*; Fraissard, J., Petrakis, L., Eds.; NATO ASI Series C; Kluwer Academic Publishers: Dordrecht, The Netherlands, 1994; Vol. 444, p 415.
- (31) Koopal, L. K.; Van Riemsdijk, W. H. *J. Colloid Interface Sci.* **1989**, 128, 188.
- (32) Westall, J. *Aquatic Surface Chemistry*; Stumm, W., Ed.; Wiley: New York, 1987.
- (33) Van Riemsdijk, W. H.; Bolt, Koopal, L. K.; G. H.; Blaakmeer, J. *J. Colloid Interface Sci.* **1986**, 109, 219.
- (34) Van Riemsdijk, W. H.; De Wit, J. C. M.; Koopal, L. K.; Bolt, G. H. *J. Colloid Interface Sci.* **1987**, 116, 511.
- (35) Healy, T. W.; White, L. R. *Adv. Colloid Interface Sci.* **1978**, 9, 303.
- (36) Huang, C. P.; Stumm, W. *J. Colloid Interface Sci.* **1973**, 43, 409.
- (37) Schindler, P. W.; Stumm, W. *Aquatic Surface Chemistry*; Stumm, W., Ed.; Wiley: New York, 1987.
- (38) Hiemstra, T.; Van Riemsdijk, W. H.; Bolt, G. H. *J. Colloid Interface Sci.* **1989**, 133, 91.
- (39) Hiemstra, T.; De Wit, J. C. M.; Van Riemsdijk, W. H. *J. Colloid Interface Sci.* **1989**, 133, 105.
- (40) Hiemstra, T.; Venema, P.; Van Riemsdijk, W. H. *J. Colloid Interface Sci.* **1996**, 184, 680.
- (41) Keizer, M. G.; Van Riemsdijk, W. H. *ECOSAT: Technical Report of the Department of Soil Science and Plant Nutrition*; Wageningen University: Wageningen, The Netherlands, 1998.
- (42) Sahai, N.; Sverjensky, D. A. *Geochim. Cosmochim. Acta* **1997**, 61, 2801.
- (43) Bourikas, K.; Hiemstra, T.; Van Riemsdijk, W. H. *Langmuir* **2001**, 17, 749.
- (44) Kosmulski, M. *Adv. Colloid Interface Sci.* **2002**, 99, 255.
- (45) Park, J.; Regalbuto, J. R. *J. Colloid Interface Sci.* **1995**, 175, 239.
- (46) Garcia, H.; Nieto, J. M. L.; Palomares, E.; Solsona, B. *Catal. Lett.* **2001**, 69, 217.
- (47) Russo, S.; Noguera, C. *Surf. Sci.* **1992**, 262, 245.
- (48) Mejias, J. A.; Berry, A. J.; Refson, K.; Fraser, D. G. *Chem. Phys. Lett.* **1999**, 314, 558.
- (49) Stumm, W.; Huang, C. P.; Jenkins, S. R. *Croat. Chem. Acta* **1970**, 42, 223.
- (50) Hayes, K. F.; Redden, G.; Ela, W.; Leckie, J. O. *J. Colloid Interface Sci.* **1991**, 142, 448.
- (51) Borkovec, M. *Langmuir* **1997**, 13, 2608.
- (52) Piasecki, W.; Rudzinski, W.; Charnas, R. *J. Phys. Chem. B* **2001**, 105, 9755.
- (53) Spanos, N.; Georgiadou, I.; Lycourghiotis, A. *J. Colloid Interface Sci.* **1995**, 172, 374.
- (54) Bourikas, K.; Matralis, H. K.; Kordulis, Ch.; Lycourghiotis, A. *J. Phys. Chem.* **1996**, 100, 11711.
- (55) Hohl, H.; Stumm, W. *J. Colloid Interface Sci.* **1976**, 55, 281.
- (56) Kummert, R.; Stumm, W. *J. Colloid Interface Sci.* **1980**, 75, 373.
- (57) Stern, O. *Z. Elektrochem.* **1924**, 30, 508.
- (58) Bowden, J. W.; Posner, A. M.; Quirk, J. P. *Aust. J. Soil. Res.* **1977**, 15, 121.
- (59) Hiemstra, T.; Yong, H.; Van Riemsdijk, W. H. *Langmuir* **1999**, 15, 5942.
- (60) Kosmulski, M.; Rosenholm, J. B. *J. Phys. Chem.* **1996**, 100, 11681.
- (61) Kosmulski, M.; Durand-Vidal, S.; Gustafsson, J.; Rosenholm, J. B. *Colloids Surf., A* **1999**, 157, 245.
- (62) Rowlands, W. N.; O'Brien, R. W.; Hunter, R. J.; Patrick, V. J. *J. Colloid Interface Sci.* **1997**, 188, 325.
- (63) Kosmulski, M.; Matijevic, E. *Colloid Polym. Sci.* **1992**, 270, 1046.